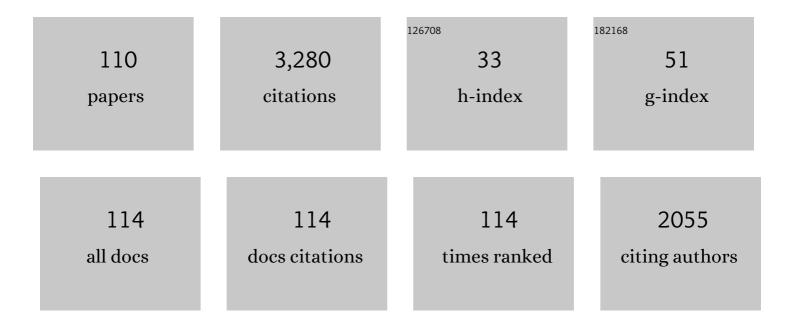
Michael R Tonks

List of Publications by Year in descending order

Source: https://exaly.com/author-pdf/3038472/publications.pdf Version: 2024-02-01



#	Article	IF	CITATIONS
1	Phase-field modeling of carbon fiber oxidation coupled with heat conduction. Computational Materials Science, 2022, 204, 111156.	1.4	4
2	Modeling mesoscale fission gas behavior in UO2 by directly coupling the phase field method to spatially resolved cluster dynamics. Materials Theory, 2022, 6, .	2.2	8
3	Assessment of four strain energy decomposition methods for phase field fracture models using quasi-static and dynamic benchmark cases. Materials Theory, 2022, 6, .	2.2	7
4	Thermal Energy Transport in Oxide Nuclear Fuel. Chemical Reviews, 2022, 122, 3711-3762.	23.0	37
5	The effect of stress on the migration of He gas bubbles under a thermal gradient in Fe by phase-field modeling. Computational Materials Science, 2022, 209, 111392.	1.4	3
6	An efficient and quantitative phase-field model for elastically heterogeneous two-phase solids based on a partial rank-one homogenization scheme. International Journal of Solids and Structures, 2022, 250, 111709.	1.3	3
7	Generation and characterization of an improved carbon fiber model by molecular dynamics. Carbon, 2021, 173, 232-244.	5.4	21
8	A CALPHAD-informed approach to modeling constituent redistribution in Zr-based metallic fuels using BISON. Journal of Nuclear Materials, 2021, 544, 152657.	1.3	14
9	Analysis of the impact of fuel microstructure on irradiation-enhanced densification using grand potential simulations. Annals of Nuclear Energy, 2021, 151, 107858.	0.9	3
10	Mechanistic grain growth model for fresh and irradiated UO2 nuclear fuel. Journal of Nuclear Materials, 2021, 543, 152576.	1.3	12
11	Comparative analysis of two isocyanate-free urethane-based gels for antifouling applications. Biofouling, 2021, 37, 131-144.	0.8	3
12	BISON: A Flexible Code for Advanced Simulation of the Performance of Multiple Nuclear Fuel Forms. Nuclear Technology, 2021, 207, 954-980.	0.7	75
13	Scalable Feature Tracking for Finite Element Meshes Demonstrated with a Novel Phase-Field Grain Subdivision Model. Nuclear Technology, 2021, 207, 885-904.	0.7	6
14	Quantifying the effect of hydride microstructure on zirconium alloys embrittlement using image analysis. Journal of Nuclear Materials, 2021, 547, 152817.	1.3	21
15	Impact of fission gas bubbles on thermal conductivity of UO <mml:math xmlns:mml="http://www.w3.org/1998/Math/MathML" altimg="si3.svg"><mml:msub><mml:mrow /><mml:mn>2</mml:mn></mml:mrow </mml:msub> fuels with high thermal conductivity additives. lournal of Nuclear Materials. 2021. 546. 152779.</mml:math 	1.3	2
16	Evolution of microstructures in radiation fields using a coupled binary-collision Monte Carlo phase field approach. Computational Materials Science, 2021, 192, 110321.	1.4	5
17	Multiscale Simulations of Thermal Transport in W-UO ₂ CERMET Fuel for Nuclear Thermal Propulsion. Nuclear Technology, 2021, 207, 1004-1014.	0.7	7
18	Modeling brittle fracture due to anisotropic thermal expansion in polycrystalline materials. Computational Materials Science, 2021, 194, 110407.	1.4	10

#	Article	IF	CITATIONS
19	Investigation of <mml:math <br="" xmlns:mml="http://www.w3.org/1998/Math/MathML">altimg="si2.svg"><mml:mi>δ</mml:mi></mml:math> zirconium hydride morphology in a single crystal using quantitative phase field simulations supported by experiments. Journal of Nuclear Materials, 2021. 557. 153303.	1.3	12
20	Review and Preliminary Investigation into Fuel Loss from Cermets Composed of Uranium Nitride and a Molybdenum-Tungsten Alloy for Nuclear Thermal Propulsion Using Mesoscale Simulations. Jom, 2021, 73, 3528-3543.	0.9	5
21	High-temperature oxidation of carbon fiber and char by molecular dynamics simulation. Carbon, 2021, 185, 449-463.	5.4	14
22	A Modified Embedded-Atom Potential for Fe-Cr-Si Alloys. Journal of Physical Chemistry C, 2021, 125, 22863-22871.	1.5	5
23	A new phase field fracture model for brittle materials that accounts for elastic anisotropy. Computer Methods in Applied Mechanics and Engineering, 2020, 358, 112643.	3.4	28
24	Development of a microstructural grand potential-based sintering model. Computational Materials Science, 2020, 172, 109288.	1.4	36
25	In search of Î,-(Pu,Zr) in binary Pu–Zr: Thermal and microstructural analyses of Pu'â^â€~30Zr alloy. Journal of Nuclear Materials, 2020, 528, 151875.	1.3	2
26	Reexamination of a U-Zr diffusion couple experiment using quantitative phase-field modeling and sensitivity analysis. Journal of Nuclear Materials, 2020, 529, 151929.	1.3	5
27	Phase-field simulations of intergranular fission gas bubble behavior in U3Si2 nuclear fuel. Journal of Nuclear Materials, 2020, 541, 152415.	1.3	17
28	Development and application of a microstructure dependent thermal resistor model for UO2 reactor fuel with high thermal conductivity additives. Journal of Nuclear Materials, 2020, 540, 152334.	1.3	5
29	The effects of introducing elasticity using different interpolation schemes to the grand potential phase field model. Computational Materials Science, 2020, 183, 109790.	1.4	8
30	Development of a grain growth model for U3Si2 using experimental data, phase field simulation and molecular dynamics. Journal of Nuclear Materials, 2020, 532, 152069.	1.3	13
31	Evaluations of the performance of multi-metallic layered composite cladding for the light water reactor accident tolerant fuel. Journal of Nuclear Materials, 2020, 535, 152136.	1.3	12
32	Grand potential sintering simulations of doped UO2 accident-tolerant fuel concepts. Journal of Nuclear Materials, 2020, 532, 152052.	1.3	17
33	Uncertainty quantification of mesoscale models of porous uranium dioxide. , 2020, , 329-354.		2
34	Development of a New Thermochemistry Solver for Multiphysics Simulations of Nuclear Materials. Minerals, Metals and Materials Series, 2020, , 1013-1025.	0.3	4
35	Microstructural characterization of the as-cast and annealed Pu-10Zr alloy. Journal of Nuclear Materials, 2019, 523, 80-90.	1.3	4
36	Mesoscale Modeling of High Burn-Up Structure Formation and Evolution in UO2. Jom, 2019, 71, 4817-4828.	0.9	14

#	Article	IF	CITATIONS
37	Phase-field modeling of fission gas bubble growth on grain boundaries and triple junctions in UO2 nuclear fuel. Computational Materials Science, 2019, 161, 35-45.	1.4	26
38	Nano- and micro-indentation testing of sintered UO2 fuel pellets with controlled microstructure and stoichiometry. Journal of Nuclear Materials, 2019, 516, 169-177.	1.3	30
39	A study of constituent redistribution in U–Zr fuels using quantitative phase-field modeling and sensitivity analysis. Journal of Nuclear Materials, 2019, 523, 143-156.	1.3	19
40	The Phase Field Method: Mesoscale Simulation Aiding Material Discovery. Annual Review of Materials Research, 2019, 49, 79-102.	4.3	44
41	Hydrogen in zirconium alloys: A review. Journal of Nuclear Materials, 2019, 518, 440-460.	1.3	203
42	The microstructure and thermodynamic behavior of as-cast U-24Pu-15Zr: Unexpected results and recommendations for U-Pu-Zr fuel research methodology. Journal of Nuclear Materials, 2019, 518, 80-94.	1.3	8
43	Development and verification of a phase-field model for the equilibrium thermodynamics of U-Pu-Zr. Annals of Nuclear Energy, 2019, 124, 490-502.	0.9	6
44	PFHub: The Phase-Field Community Hub. Journal of Open Research Software, 2019, 7, 29.	2.7	7
45	How to apply the phase field method to model radiation damage. Computational Materials Science, 2018, 147, 353-362.	1.4	31
46	Phase field modeling of sintering: Role of grain orientation and anisotropic properties. Computational Materials Science, 2018, 148, 307-319.	1.4	42
47	Implementation of a phase field model for simulating evolution of two powder particles representing microstructural changes during sintering. Journal of Materials Science, 2018, 53, 5799-5825.	1.7	34
48	Review of sintering and densification in nuclear fuels: Physical mechanisms, experimental results, and computational models. Journal of Nuclear Materials, 2018, 507, 381-395.	1.3	21
49	Theoretical prediction and atomic kinetic Monte Carlo simulations of void superlattice self-organization under irradiation. Scientific Reports, 2018, 8, 6629.	1.6	27
50	Unit mechanisms of fission gas release: Current understanding and future needs. Journal of Nuclear Materials, 2018, 504, 300-317.	1.3	80
51	Radiation-induced grain subdivision and bubble formation in U3Si2 at LWR temperature. Journal of Nuclear Materials, 2018, 498, 169-175.	1.3	25
52	In-situ TEM study of the ion irradiation behavior of U3Si2 and U3Si5. Journal of Nuclear Materials, 2018, 511, 56-63.	1.3	12
53	Grand-potential-based phase-field model for multiple phases, grains, and chemical components. Physical Review E, 2018, 98, 023309.	0.8	40
54	Sintering And Densification In Nuclear Power. , 2018, , .		0

#	Article	IF	CITATIONS
55	Particle-grain boundary interactions: A phase field study. Computational Materials Science, 2017, 134, 25-37.	1.4	22
56	Mechanistic materials modeling for nuclear fuel performance. Annals of Nuclear Energy, 2017, 105, 11-24.	0.9	57
57	Quantifying elastic energy effects on interfacial energy in the Kim-Kim-Suzuki phase-field model with different interpolation schemes. Computational Materials Science, 2017, 140, 10-21.	1.4	26
58	Formation path of δ hydrides in zirconium by multiphase field modeling. Acta Materialia, 2017, 123, 235-244.	3.8	45
59	Quantitative polynomial free energy based phase field model for void motion and evolution in Sn under thermal gradient. , 2017, , .		1
60	Molecular dynamics simulations of concentration-dependent defect production in Fe-Cr and Fe-Cu alloys. Journal of Applied Physics, 2017, 122, 225902.	1.1	11
61	Homogeneous hydride formation path in $\hat{I}\pm$ -Zr: Molecular dynamics simulations with the charge-optimized many-body potential. Acta Materialia, 2016, 111, 357-365.	3.8	35
62	A phase-field model to study the effects of temperature change on shape evolution of <i>γ</i> -hydrides in zirconium. Journal Physics D: Applied Physics, 2016, 49, 405302.	1.3	14
63	Development of a multiscale thermal conductivity model for fission gas in UO2. Journal of Nuclear Materials, 2016, 469, 89-98.	1.3	63
64	Order parameter re-mapping algorithm for 3D phase field model of grain growth using FEM. Computational Materials Science, 2016, 115, 18-25.	1.4	47
65	Multi-scale modeling of microstructure dependent intergranular brittle fracture using a quantitative phase-field based method. Computational Materials Science, 2016, 113, 38-52.	1.4	67
66	Multiscale modeling of thermal conductivity of high burnup structures in UO2 fuels. Journal of Nuclear Materials, 2016, 470, 208-215.	1.3	50
67	A study of the evolution of microstructure and consolidation kinetics during sintering using a phase field modeling based approach. Extreme Mechanics Letters, 2016, 7, 78-89.	2.0	65
68	Development of a grain boundary pinning model that considers particle size distribution using the phase field method. Modelling and Simulation in Materials Science and Engineering, 2015, 23, 045009.	0.8	49
69	Preferential Cu precipitation at extended defects in bcc Fe: An atomistic study. Computational Materials Science, 2015, 101, 181-188.	1.4	17
70	A review on hydride precipitation in zirconium alloys. Journal of Nuclear Materials, 2015, 466, 12-20.	1.3	109
71	Multiscale simulation of xenon diffusion and grain boundary segregation in UO2. Journal of Nuclear Materials, 2015, 462, 15-25.	1.3	32
72	Formation of prismatic loops from C15 Laves phase interstitial clusters in body-centered cubic iron. Scripta Materialia, 2015, 98, 5-8.	2.6	44

#	Article	IF	CITATIONS
73	Testing thermal gradient driving force for grain boundary migration using molecular dynamics simulations. Acta Materialia, 2015, 85, 95-106.	3.8	32
74	Physics-based multiscale coupling for full core nuclear reactor simulation. Annals of Nuclear Energy, 2015, 84, 45-54.	0.9	184
75	Using Coupled Mesoscale Experiments and Simulations to Investigate High Burn-Up Oxide Fuel Thermal Conductivity. Jom, 2014, 66, 2569-2577.	0.9	18
76	Demonstrating the Temperature Gradient Impact on Grain Growth in UO2Using the Phase Field Method. Materials Research Letters, 2014, 2, 23-28.	4.1	38
77	Microstructural modeling of thermal conductivity of high burn-up mixed oxide fuel. Journal of Nuclear Materials, 2014, 444, 161-169.	1.3	21
78	Modeling the influence of bubble pressure on grain boundary separation and fission gas release. Journal of Nuclear Materials, 2014, 452, 95-101.	1.3	19
79	Molecular dynamics simulations of intergranular fracture in UO2 with nine empirical interatomic potentials. Journal of Nuclear Materials, 2014, 452, 296-303.	1.3	37
80	Strain effects on oxygen transport in tetragonal zirconium dioxide. Physical Chemistry Chemical Physics, 2013, 15, 19438.	1.3	37
81	Consideration of grain size distribution in the diffusion of fission gas to grain boundaries. Journal of Nuclear Materials, 2013, 440, 435-439.	1.3	6
82	Three dimensional calculations of the effective Kapitza resistance of UO2 grain boundaries containing intergranular bubbles. Journal of Nuclear Materials, 2013, 439, 117-122.	1.3	26
83	A quantitative comparison between and elements for solving the Cahn–Hilliard equation. Journal of Computational Physics, 2013, 236, 74-80.	1.9	35
84	Guidance to design grain boundary mobility experiments with molecular dynamics and phase-field modeling. Acta Materialia, 2013, 61, 1373-1382.	3.8	15
85	Multiscale development of a fission gas thermal conductivity model: Coupling atomic, meso and continuum level simulations. Journal of Nuclear Materials, 2013, 440, 193-200.	1.3	35
86	Compositional patterning in immiscible alloys subjected to severe plastic deformation. Journal of Materials Research, 2013, 28, 2687-2693.	1.2	18
87	Molecular dynamics simulations of He bubble nucleation at grain boundaries. Journal of Physics Condensed Matter, 2012, 24, 305005.	0.7	15
88	Parallel Algorithms and Software for Nuclear, Energy, and Environmental Applications. Part II: Multiphysics Software. Communications in Computational Physics, 2012, 12, 834-865.	0.7	12
89	An object-oriented finite element framework for multiphysics phase field simulations. Computational Materials Science, 2012, 51, 20-29.	1.4	217
90	Phase-field modeling of temperature gradient driven pore migration coupling with thermal conduction. Computational Materials Science, 2012, 56, 161-165.	1.4	38

#	Article	IF	CITATIONS
91	Deformation twins in nanocrystalline body-centered cubic Mo as predicted by molecular dynamics simulations. Acta Materialia, 2012, 60, 6421-6428.	3.8	36
92	Crack tip plasticity in single crystal UO2: Atomistic simulations. Journal of Nuclear Materials, 2012, 430, 96-105.	1.3	29
93	Random-walk Monte Carlo simulation of intergranular gas bubble nucleation in UO2 fuel. Journal of Nuclear Materials, 2012, 430, 44-49.	1.3	6
94	Mesoscale modeling of intergranular bubble percolation in nuclear fuels. Journal of Applied Physics, 2012, 111, .	1.1	9
95	Deformation-twin-induced grain boundary failure. Scripta Materialia, 2012, 66, 117-120.	2.6	54
96	Phase-field simulation of intergranular bubble growth and percolation in bicrystals. Journal of Nuclear Materials, 2012, 425, 130-135.	1.3	42
97	Atomistic study of grain boundary sink strength under prolonged electron irradiation. Journal of Nuclear Materials, 2012, 422, 69-76.	1.3	40
98	Grain boundary percolation modeling of fission gas release in oxide fuels. Journal of Nuclear Materials, 2012, 424, 176-182.	1.3	23
99	Phase-field simulation of irradiated metals. Computational Materials Science, 2011, 50, 949-959.	1.4	83
100	Phase-field simulations of gas density within bubbles in metals under irradiation. Computational Materials Science, 2011, 50, 2044-2050.	1.4	17
101	Energetics and diffusional properties of He in BCC Mo: An empirical potential for molecular dynamics simulations. Computational Materials Science, 2011, 50, 3224-3229.	1.4	8
102	Application of phase-field modeling to irradiation effects in materials. Current Opinion in Solid State and Materials Science, 2011, 15, 125-133.	5.6	37
103	Meso-scale modeling of the influence of intergranular gas bubbles on effective thermal conductivity. Journal of Nuclear Materials, 2011, 412, 281-286.	1.3	46
104	Phase field simulations of elastic deformation-driven grain growth in 2D copper polycrystals. Materials Science & Engineering A: Structural Materials: Properties, Microstructure and Processing, 2011, 528, 4086-4091.	2.6	34
105	Analysis of the elastic strain energy driving force for grain boundary migration using phase field simulation. Scripta Materialia, 2010, 63, 1049-1052.	2.6	42
106	A coupling methodology for mesoscale-informed nuclear fuel performance codes. Nuclear Engineering and Design, 2010, 240, 2877-2883.	0.8	16
107	Atomistic simulations of void migration under thermal gradient in UO2. Acta Materialia, 2010, 58, 330-339.	3.8	24
108	Two stochastic mean-field polycrystal plasticity methods. Journal of the Mechanics and Physics of Solids. 2009. 57, 1230-1253.	2.3	9

#	Article	IF	CITATIONS
109	Void nucleation and growth in irradiated polycrystalline metals: a phase-field model. Modelling and Simulation in Materials Science and Engineering, 2009, 17, 064003.	0.8	65
110	A design of inverse Taylor projectiles using material simulation. Modelling and Simulation in Materials Science and Engineering, 2008, 16, 015005.	0.8	0